Liquid Crystals
Publication details, including instructions for authors and subscription information:
http://www.informaworld.com/smpp/title~content=t713926090

Supramolecular side chain liquid crystalline polymers assembled via hydrogen bonding between carboxylic acid-containing polysiloxane and azobenzene derivatives

Suat Hong Goh; Yee Hing Lai; Si Xue Cheng

Online publication date: 06 August 2010

To cite this Article Goh, Suat Hong , Lai, Yee Hing and Cheng, Si Xue(2001) 'Supramolecular side chain liquid crystalline polymers assembled via hydrogen bonding between carboxylic acid-containing polysiloxane and azobenzene derivatives', Liquid Crystals, 28: 10, 1527 — 1538
To link to this Article: DOI: 10.1080/02678290110071556
URL: http://dx.doi.org/10.1080/02678290110071556

LIQUID CRYSTALS, 2001, VOL. 28, NO. 10, 1527–1538

Supramolecular side chain liquid crystalline polymers assembled via hydrogen bonding between carboxylic acid-containing polysiloxane and azobenzene derivatives

XU LI, SUAT HONG GOH*, YEE HING LAI

Department of Chemistry, National University of Singapore, 3 Science Drive 3, Singapore 117543

and SI XUE CHENG

Institute of Materials and Engineering, National University of Singapore, 3 Research Link, Singapore 117602

(*Received 11 January 2001; accepted 15 May 2001*)

Supramolecular side chain liquid crystalline polymers were prepared from poly(3-carboxypropylmethylsiloxane) (PSI100) and azobenzene derivatives through intermolecular hydrogen bonding (H-bonding) between the carboxylic acid groups in the PSI100 and the imidazole rings in the azobenzene derivatives. The existence of H-bonding has been confirmed using FTIR spectroscopy. The polymeric complexes behave as liquid crystalline (LC) polymers and exhibit stable mesophases. The LC behaviour of these H-bonded polymeric complexes was investigated by differential scanning calorimetry, polarizing optical microscopy and X-ray diffraction. The complexes exhibit nematic LC phases identified on the basis of Schlieren optical textures. On increasing spacer length or the concentration of the H-bonded mesogenic unit in the complex, the clearing temperature and the temperature range of the LC phase of the polymeric complex increase. The terminal group plays a critical role in determining the LC properties of the polymeric complexes. A terminal methoxy group is more efficient than a nitro group in increasing the clearing temperature. The electron donor–acceptor interactions between the H-bonded mesogenic units containing methoxy and nitro terminal groups in supramolecular 'copolymeric' complexes lead to an increase in the clearing temperature and a wider temperature range for the LC phase.

1. Introduction

In recent years side chain liquid crystalline polymers (SCLCPs), which combine properties characteristic of polymers with those of conventional low molar mass mesogens, have been the subject of intensive research. This duality of properties endows upon this class of materials application potential in various fields, ranging from optical data storage [1–4] and non-linear optics [5–8] to being the stationary phase in gas chromatography [9, 10] and high performance liquid chromatography [11, 12]. SCLCPs are generally prepared by covalently linking rigid mesogens to polymer backbones through flexible spacers. The function of the spacer is to decouple the motions of the polymer backbone from the self-ordering tendencies of the mesogens. In recent years, self-assembly through specific interactions, such as hydrogen bonding (H-bonding) [13–26], ionic [27–29], ionic–dipolar [30, 31] and charge transfer interactions [32, 33], has been recognized as a new strategy for constructing SCLCPs. Because of their simplicity of preparation, these self-assembled SCLCPs have the advantage of being able to fine tune the liquid crystalline properties. Various molecular parameters, such as the nature of the rigid cores, the nature and the length of the terminal groups, and the spacer length, can be modified with relative ease compared with covalently-bonded systems. Another advantage of self-assembled SCLCPs is the ease with which various 'copolymers' can be prepared through the simple mixing of the polymer and different low molar mass mesogens.

The H-bonding interaction is one of the most important and widely used non-covalent interaction in the design and construction of supramolecular architectures. Carboxylic and benzoic acid groups are widely used as H-bond donors while pyridine moieties are commonly used as H-bond acceptors. Complexes obtained through

*Author for correspondence; e-mail: chmgohsh@nus.edu.sg

Liquid Crystals ISSN 0267-8292 print/ISSN 1366-5855 online © 2001 Taylor & Francis Ltd
http://www.tandf.co.uk/journals
DOI: 10.1080/02678290110071556

intermolecular H-bonding include systems consisting of derivatives of carboxylic (or benzoic) acid/pyridine [13–21], carboxylic acid/2,6-diaminopyridine [22, 23], uracil/2,6-diaminopyridine [24, 25] and carboxylic acid/pyridine *N*-oxide [26]. Many biological processes in nature involve the participation of imidazoyl groups. Imidazole derivatives are useful as H-bonding components in connecting different molecular parts through the formation of stable H-bonds. We have studied the interactions in blends or complexes of poly(1-vinylimidazole) and some H-bond donor polymers, such as poly(3-carboxypropylmethylsiloxane) [34], poly(acrylic acid) [35] and poly(*p*-vinylphenol) [35]. We have shown that the imidazole nitrogen is a better electron-pair donor than the pyridine nitrogen. As a result, the H-bond formed with the imidazole group is stronger than that with the pyridine group. To our knowledge, only Kawakami and Kato [15] have studied supramolecular complexes formed through H-bonding between poly(acrylic acid) and imidazoyl moieties. The various H-bonded complexes exhibit smectic A phases.

In the present study, several mesogenic azobenzene derivatives are attached to a polysiloxane-based backbone through H-bond interactions between the carboxylic acid groups in poly(3-carboxypropylmethylsiloxane) (PSI100) and the imidazole rings in the azobenzene derivatives. The results obtained from differential scanning calorimetry (DSC), polarizing optical microscopy (POM) and X-ray diffraction (XRD) show that the mesogenic properties of the supramolecular complexes are dependent on the spacer length, the nature of the terminal group and the composition of the complexes. The flexible polysiloxane backbone enables the formation of a liquid crystalline phase near room temperature.

2. Experimental

2.1. *Materials*

(3-Cyanopropyl)methyldichlorosilane, *p*-nitroaniline, aniline, imidazole and phenol were supplied by Fluka Chemika-Biochemika. Poly(dimethylsiloxane) (PDMS) with a viscosity of 60 000 cSt, *p*-anisidine, 1,6-dibromohexane, 1,4-dibromobutane and potassium carbonate were supplied by Aldrich Chemical Co. All the chemicals were used as received. Tetrahydrofuran (THF) was dried by heating at reflux with sodium in a nitrogen atmosphere. Acetone was dried over molecular sieve (4 Å). 4-Hydroxy-4′-nitroazobenzene and 1-bromo-6-(4-nitroazobenzene-4′-oxy)hexane were prepared following the procedures reported by Imrie *et al.* [36].

2.2. *Synthesis of carboxylic acid-containing polysiloxane*

The synthesis and characterization of PSI100 were reported previously [37]. PSI100 shows an initial decomposition temperature at 210°C, as shown by thermogravimetric analysis. The number-average molecular mass of PSI100 is 6.6×10^3 g mol^{-1} and the polydispersity is 1.6; its glass transition temperature is −9°C.

2.3. *Synthesis of 4-nitro-4′-[6-(imidazole-1-yl)-hexyloxy]azobenzene (NO6I)*

A mixture of 1-bromo-6-(4-nitroazobenzene-4′-oxy)-hexane (4.06 g, 0.01 mol), imidazole (1.02 g, 0.015 mol) and potassium carbonate (2.76 g, 0.02 mol) in dry THF (100 ml) was heated at reflux with stirring for 24 h under a nitrogen atmosphere. After the addition of dichloromethane (100 ml), the solution was filtered to remove salts. After the removal of THF and dichloromethane, the crude product was purified using a silica gel column with dichloromethane/methanol (30:1) as eluent. ^{1}H NMR ($CDCl_3$, ppm): 8.35–8.38 (2H, NO_2−Ar−H), 7.95–8.00 (4H, N=N−Ar−H), 7.00–7.03 (2H, O-Ar−H), 7.47, 7.06, 6.91 (3H, imidazoyl), 4.03–4.07 (2H, Ar−O−CH_2), 3.94–3.98 (2H, Im−CH_2), 1.79–1.86 (4H, Ar−O−C−CH_2, Im−C−CH_2), 1.51–1.56 (2H, Im−C−C−C−CH_2−C−C−O), 1.36–1.44 (2H, Im−C−C−CH_2−C−C−C−O−Ar). Anal: calcd for $C_{21}H_{23}N_5O_3$ C 64.12, H 5.85, N 17.81; found C 64.59, H 5.59, N 18.00%.

4-Nitro-4′-[4-(imidazole-1-yl)butyloxy]azobenzene (NO4I), 4-methoxy-4′-[6-(imidazole-1-yl)hexyloxy]azobenzene (MEO6I), 4-methoxy-4′-[4-(imidazole-1-yl)-butyloxy]azobenzene (MEO4I), 4-[6-(imidazole-1-yl)-hexyloxy]azobenzene (H6I) and 4-[4-(imidazole-1-yl)-butyloxy]azobenzene (H4I) were prepared according to the method for the preparation of NO6I.

2.4. *Characterization*

^{1}H NMR spectra were recorded on a Bruker ACF 300 spectrometer at 25°C with TMS as an internal standard. FTIR spectra were recorded on a Bio-Rad 165 FTIR spectrophotometer; 64 scans were signal-averaged with a resolution of 2 cm^{-1}. Samples were prepared by dispersing the complexes in KBr and compressing the mixtures to form disks. Spectra were recorded at a specific temperature, using a Specac high temperature cell equipped with an automatic temperature controller, mounted in the spectrophotometer.

DSC was performed using a TA Instruments 2920 differential scanning calorimeter equipped with an autocool accessory and calibrated using indium. The following protocol was used for each sample: heating from room temperature to 150°C at 20°C min^{-1}, holding at 150°C for 3 min, cooling from 150°C to −30°C at 10°C min^{-1} and finally reheating from −30°C to 150°C at 10°C min^{-1}. Data were collected during the first cooling segment from the isotropic phase and the subsequent second heating segment to the isotropic phase. Transition temperatures were taken to correspond with the peak maximum.

The mesophase textures of the complexes and the pure azobenzene derivatives were observed under an Olympus BX50 polarizing optical microscope (magnification 400×) equipped with a Linkam THMS-600 hotstage which was controlled by a central processor. The software used in the image processing was Image-pro plus 3.0. The sample was pressed between a glass slide and a cover slip and observed in the LC temperature range. The heating/cooling rate was 2°C min^{-1}.

XRD was carried out using a Simens D5005 Diffractometer (40 kV, 30 mA) and Ni-filtered Cu K_α radiation in 0.01° steps from 1.5° to 40° (in 2θ) with 1 s per step. The intensity of the diffracted X-ray from the samples was measured by a scintillation counter. The samples were first heated to their isotropization temperatures, then cooled to specific temperatures gradually prior to XRD studies. Bragg's equation was used to calculate the layer spacing corresponding to the various reflections.

2.5. *Preparation of hydrogen-bonded complexes*

All hydrogen-bonded complexes were prepared by solution casting using THF as solvent. THF was removed by slow evaporation at room temperature followed by drying *in vacuo* for 2 weeks at 60°C. Unless otherwise stated, the complex contains an equimolar ratio of carboxylic acid and imidazole groups.

'Copolymeric' complexes were prepared using PSI100 and two different azobenzene derivatives by maintaining a 1:1 stoichiometry between the carboxylic acid group in PSI100 and the imidazole group in the mixture of the different azobenzene derivatives.

3. Results and discussion

3.1. *Formation of hydrogen-bonded side chain liquid crystalline polymers*

The molecular structures of the components are shown in scheme 1.

H-bond polymeric donor

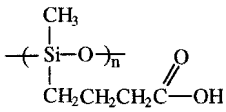

H-bond acceptors

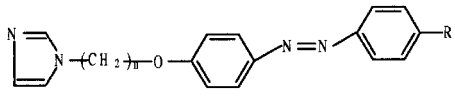

NO6I, $n=6$, $R=NO_2$; NO4I, $n=4$, $R=NO_2$
MEO6I, $n=6$, $R=OCH_3$; MEO4I, $n=4$, $R=OCH_3$
H6I, $n=6$, $R=H$; H4I, $n=4$, $R=H$

Scheme 1.

The structure of the side chain liquid crystalline polymer formed by intermolecular H-bonding between the carboxylic acid in PSI100 and the imidazole ring in NO6I is depicted below:

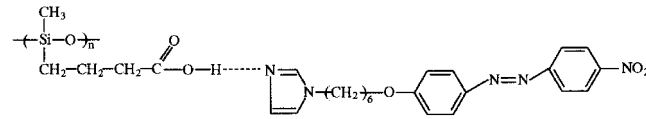

The thermal behaviour of NO6I and its complexes with PSI100 or PDMS was studied using DSC. Figure 1 shows the DSC traces of pure NO6I and its complexes; the transition temperatures and associated enthalpy changes (ΔH) are listed in table 1.

The first cooling run of NO6I, figure 1 (*a*), shows only one exothermic peak at 51°C with an associated enthalpy change of 15.85 kJ mol^{-1}. This corresponds to the crystallization of NO6I from the isotropic phase. In the second heating run of NO6I, figure 1 (*a*′), there is a cold crystallization peak at *ca.* 37°C ($\Delta H = 8.55$ kJ mol^{-1}) followed by an endothermic peak at around 100°C ($\Delta H = 32.22$ kJ mol^{-1}), which is attributed to the crystal–isotropic transition. This assignment is based on the results of POM and XRD measurements, which will be discussed later. The difference between the crystallization and melting temperatures is due to supercooling effects.

The PDMS/NO6I complex shows similar phase transition behaviour to that of pure NO6I, except for the appearance of two overlapping exothermic peaks in the first cooling run and a lower melting temperature in the second heating run. On cooling, the appearance of two overlapping peaks at 56 and 51°C with enthalpy changes of 4.62 and 1.69 kJ mol^{-1}, respectively, is due

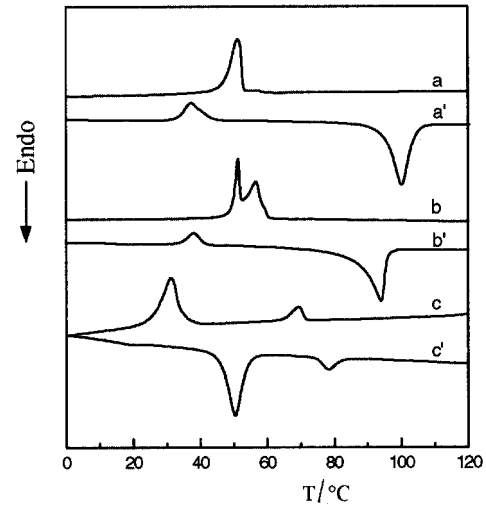

Figure 1. DSC traces of pure NO6I and its complexes. First cooling run: (*a*) NO6I, (*b*) PDMS/NO6I, (*c*) PSI100/NO6I. Second heating run: (*a*′) NO6I, (*b*′) PDMS/NO6I, (*c*′) PSI100/NO6I.

Table 1. Transition temperatures (°C) and associated enthalpy changes (kJ mol^{-1}, in parentheses) of NO6I and its complexes. I = isotropic phase; Cr = crystalline phase; N = nematic phase.

	1st cooling	2nd heating
NO6I	I 51(15.85) Cr	37(8.55)[a] Cr 100(32.22) I
PDMS/NO6I	I 56(4.62) Cr_1 51(1.69) Cr_2	34(3.32)[a] Cr 94(24.94) I
PSI100/NO6I	I 71(1.43) N 31(9.07) Cr	g 15 Cr 50(8.96) N 78(1.41) I

[a] Cold crystallization.

to the formation of two types of crystal phase. The lowering of the melting temperature in the second heating run arises from the diluting effect of the PDMS on the degree of order in the crystal. The complex did not show any birefringence when examined by POM. The similar thermal behaviour exhibited by NO6I and the PDMS/NO6I complex indicates the absence of any specific interactions between NO6I and PDMS.

Figures 1(*c*) and 1(*c*′) are the DSC curves for the PSI100/NO6I complex. As compared with the DSC trace of pure NO6I, that of the PDMS/NO6I complex on cooling, a new exothermic peak appeared at 71°C (T_{IN}) with an enthalpy change of 1.43 kJ mol^{-1}, corresponding to the transition from the isotropic phase to a liquid crystalline phase. Another exothermic peak is found at 31°C (T_{Cr}) with an enthalpy change of 9.07 kJ mol^{-1}, which is assigned to the crystallization of the complex from the mesophase. Two endothermic peaks at 50 and 78°C are observed in the second heating run. One is due to the melting of the crystal and the other to the isotropization of the liquid crystal phase. The reversible nature of the peak near 71°C during the heat–cool cycle is indicative of a phase transition between the isotropic phase and a liquid crystalline phase. POM and XRD measurements show that the complex forms a nematic phase in the temperature range between the melting temperature (T_m) and the isotropization temperature (T_{NI}). The DSC results indicate that this complex prepared from two different non-mesogenic components behaves as a single mesogenic compound. The intermolecular H-bond between the imidazole ring in NO6I and the carboxylic acid group in PSI100 gives rise to a supramolecular SCLCP which exhibits a nematic phase. Interestingly, conventional SCLCPs with a similar structure (see scheme 2) show a smectic phase with a higher degree of order [38]. The interaction between the non-covalently assembled mesogenic units is presumably not sufficiently strong to drive the microphase separation needed for smectic phase formation.

The formation of an intermolecular H-bond is shown by FTIR measurements, which reveal that the acid dimer in PSI100 is replaced by the complex. Figure 2 shows the FTIR spectra of PSI100, NO6I and their complexes.

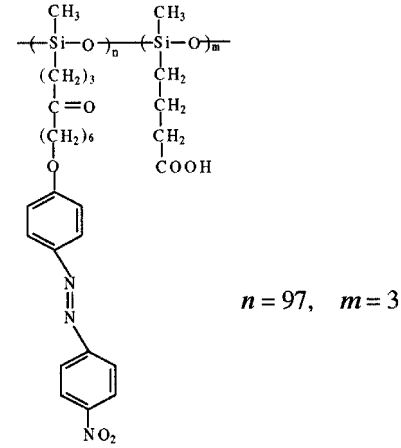

Scheme 2.

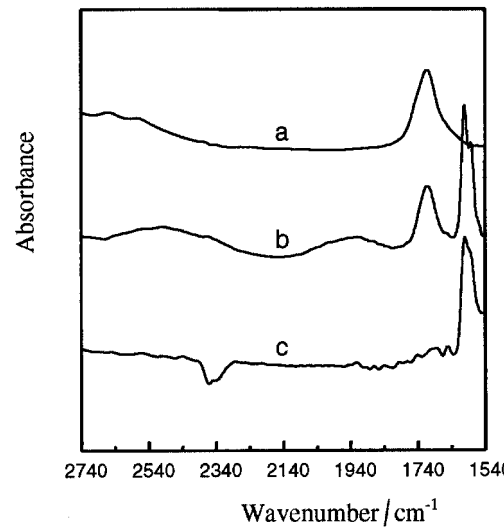

Figure 2. FTIR spectra of (*a*) PSI100, (*b*) PSI100/NO6I (1 : 1), and (*c*) NO6I.

Upon mixing PSI100 with NO6I, the broad carbonyl stretching band at around 1710 cm^{-1} becomes sharper and the peak maximum moves to a higher wave number. The changes are consistent with the liberation of carbonyl groups from the carboxylic acid dimer when PSI100 interacts with NO6I. The satellite band at around 2620 cm^{-1} attributed to the dimeric carboxylic acid groups shifts towards a lower wave number. A weak

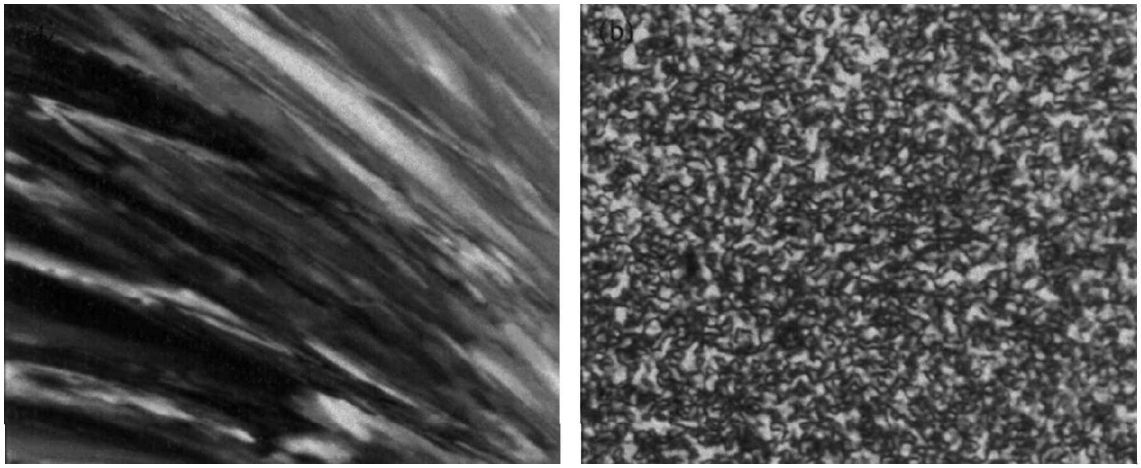

Figure 3. Optical micrographs of (*a*) pure NO6I and (*b*) the complex PSI100/NO6I: magnification 400×.

broad band centred around 1930 cm^{-1} appears, indicating the formation of a strong intermolecular H-bond between the carboxylic acid group in PSI100 and the imidazole ring in NO6I. We have studied the interaction between PSI100 and poly(1-vinylimidazole) (PVI) [34]. The appearance of the anti-symmetric vibration band of COO in the 1550–1600 cm^{-1} region, and the shift of the stretching vibration of C−C and C−N of PVI from 1500 to 1573 and 1544 cm^{-1}, respectively, upon protonation of the imidazole ring, indicate the existence of ionic interactions between PSI100 and PVI. X-ray photoelectron spectroscopic studies also confirm the existence of ionic interactions. However, in the PSI100/NO6I complex, these peaks were not found in the FTIR spectra, indicating that the interaction is H-bonding and not ionic. The difference in the nature of the interaction between that in the PSI100/PVI system [34] and the present system arises from the solvent effect. An ethanol/water (1 : 1 v/v) mixture was used for the PSI100/PVI system whereas THF was used in the present study. PSI100 ionizes more readily in the ethanol/water mixture (pH = 3.54 for a 1.0 wt % solution) than in THF (pH = 5.60 for a 1.0 wt % solution), enabling the protonation of PVI.

3.2. *Textures of hydrogen-bonded side chain liquid crystalline polymers*

To confirm the liquid crystalline nature of these complexes and to identify the phases, hot-stage polarizing optical microscopy (POM) was employed. On cooling the complexes from the isotropic phase, a birefringent texture developed when viewed through the polarizing microscope. In order to obtain a clear characteristic optical texture for phase identification, the complex was cooled slowly from approximately 20°C above its isotropization temperature at 2°C min^{-1} prior to analysis. Figure 3 shows photomicrographs of pure NO6I and the PSI100/NO6I complex under crossed polarizers. For NO6I, a texture characteristic of a crystal formed quickly at 50°C from the isotropic phase and no further change was observed on cooling. By comparison, for the PSI100/NO6I complex, a Schlieren texture developed slowly on cooling from the isotropic phase, verifying that the complex forms a nematic phase in the temperature region between T_{IN} and T_{Cr}. Similar textures were observed for other complexes. These results demonstrate clearly that nematic SCLCPs have been built through intermolecular H-bonding.

3.3. *X-ray diffraction studies*

The XRD patterns obtained for pure NO6I and the PSI100/NO6I complex in an annealed state are shown in figure 4. The XRD pattern at room temperature indicates a crystal phase for pure NO6I, figure 4 (*a*);

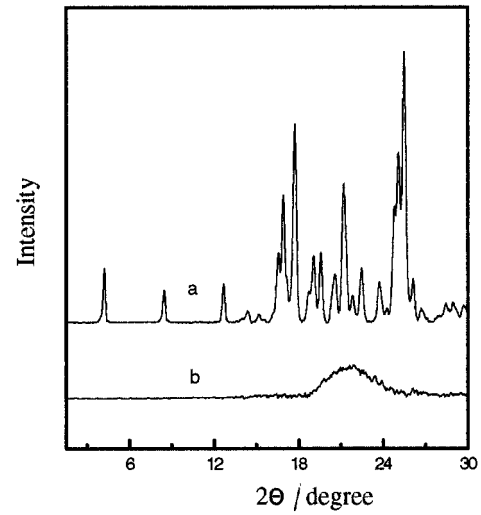

Figure 4. XRD patterns of (*a*) pure NO6I at 25°C and (*b*) the complex PSI100/NO6I at 40°C.

specifically, a number of sharp peaks are observed in both the low angle and the high angle regions. While the peaks in the low angle region are due to a layer-like structure, the sharp high angle maxima indicate an ordered structure within the layer. Upon complexation with PSI100, there is a significant change in the XRD pattern of the PSI100/NO6I complex. No diffraction maxima in either the low or the high Bragg angle region were observed, figure 4 (*b*). Only one diffuse halo at 21.5° corresponding to a *d* value of 4.1 Å was observed. This result shows that the PSI100/NO6I complex exhibits only a nematic phase. The *d* value of 4.1 Å is ascribed to the intermolecular spacing of the mesogenic units in the nematic phase.

3.4. *Effects of complex composition, spacer length and terminal group*

Figure 5 shows the DSC traces for the first cooling and second heating runs of the PSI100/NO6I complexes of varying compositions. The corresponding transition temperatures and enthalpy changes are listed in table 2. The complexes appear miscible over the entire composition range when viewed through the microscope. As can be seen in figure 5, when the molar ratio of NO6I to the carboxylic acid group in PSI100 in the complex increases from 0.4 to 1.0, the T_{IN} temperature and the enthalpy change increase from 46°C and 0.34 kJ mol^{-1} to 71°C and 1.43 kJ mol^{-1}, respectively. Therefore, the thermal stability of the mesogenic phase increases with increasing NO6I content in the complex. The formation of these supramolecular SCLCPs arises from the assembly of low molar mass compounds to the polymer backbone through H-bond interactions between the imidazole ring in the NO6I and the carboxylic acid groups in PSI100. The connection of the mesogenic unit to the polymer backbone increases the stiffness of the polymer backbone, which in turn hinders the movement of the mesogenic units and thus facilitates the packing of the mesogenic units along a specific direction. When the feed ratio is below 1.0, the higher the molar ratio of NO6I the more hydrogen-bonded mesogenic units there are in the complex and the higher is the isotropization temperature. The increase in the stiffness of the polymer backbone is shown by the change of T_g from −13°C at a molar ratio of 0.4 to 15°C at a molar ratio of 1.0. This indicates that the chemical nature of the main chain still affects the mesogenic behaviour. In other words, the motions of the main chain and the side groups are still coupled despite the presence of spacer groups between them.

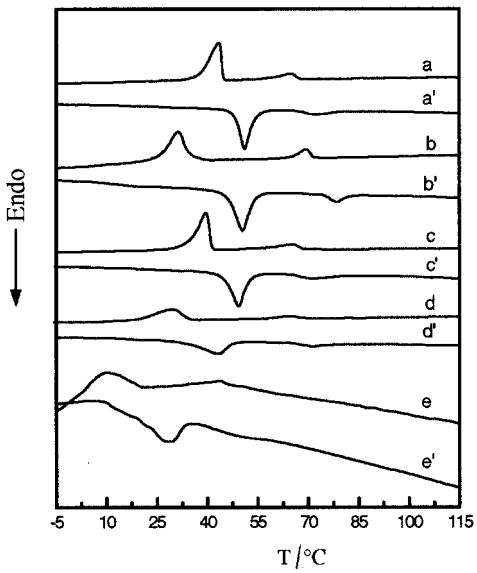

Figure 5. DSC traces of PSI100/NO6I complexes of different molar ratios. First cooling run: (*a*) 1 : 1.2, (*b*) 1 : 1, (*c*) 1 : 0.8, (*d*) 1 : 0.6, (*e*) 1 : 0.4. Second heating run: (*a'*) 1 : 1.2, (*b'*) 1 : 1, (*c'*) 1 : 0.8, (*d'*) 1 : 0.6, (*e'*) 1 : 0.4.

For the present system, the various PSI100/NO6I complexes can be regarded as copolymers of H-bonded mesogenic units and non-mesogenic units containing the carboxylic acid groups. As the carboxylic acid groups are attached to the main chain covalently through three methylene units, it is unlikely that they form stable rings along the polymer backbone. Since the carboxylic acid groups are not liquid crystalline, they play the role of a 'diluent' of the LC phase in the complex, leading to a decrease in thermal stability of the mesophase. As a result, increasing the concentration of the carboxylic acid groups in the complex will lead to a decrease in

Table 2. Transition temperatures (°C) and associated enthalpy changes (kJ mol^{-1}, in parentheses) of PSI100/NO6I complexes of varying composition. I = isotropic phase; Cr = crystalline phase; N = nematic phase; g = glassy phase.

Mol ratio (PSI100 : NO6I)	1st cooling	2nd heating
1 : 0.4	I 46(0.34) N 10(1.29) Cr	g −13 Cr 26(1.88) N 48(0.25) I
1 : 0.6	I 64(0.83) N 30(4.92) Cr	g −9 Cr 43(5.20) N 71(0.84) I
1 : 0.8	I 66(1.32) N 40(8.1) Cr	g 3 Cr 50(7.86) N 72(1.25) I
1 : 1.0	I 71(1.43) N 31(9.07) Cr	g 15 Cr 50(8.96) N 78(1.41) I
1 : 1.2	I 65(1.40) N 43(11.96) Cr	g 20 Cr 51(11.31) N 72(1.38) I

T_{IN}. The formation of a SCLCP at a molar ratio of 0.4 indicates that the H-bonded NO6I at such a level is sufficient for the formation of a LC phase.

When the molar ratio of NO6I to the carboxylic acid groups is above 1.0, there are insufficient carboxylic acid groups to ensure a one-to-one interaction. Some of the NO6I cannot be connected to the main chain through H-bonding, although the excess NO6I can be incorporated into the LC phase through dipolar interactions between the NO6I molecules. Thus, the excess NO6I molecules disrupt the ordering within the LC phase, and the transition temperature and enthalpy change both decrease. For all complexes, even when the molar ratio is as high as 1.2, phase separation is not observed optically. This composition-dependent thermal stability of the LC phase may be attributed to the higher degree of cooperative intermolecular interaction and to the paired mesogen effect at a higher concentration of the hydrogen-bonded species.

For SCLCPs, the spacer between the polymer backbone and the mesogenic side group plays an important role in determining the mesogenic properties of the polymer. The function of the spacer is to decouple the motions of the polymer backbone, which tends to form a random coil, from those of the mesogenic groups that are ordered in the liquid crystalline state. The thermal properties of the equimolar complexes of PSI100/MEO6I, PSI100/MEO4I, PSI100/NO6I and PSI100/NO4I are shown in figure 6. For the PSI100/MEO6I complex, there is only one exothermic peak at 83°C with an enthalpy change of 3.44 kJ mol^{-1} in the cooling run (*a*), and one endothermic peak at 91°C with an enthalpy change of 3.23 kJ mol^{-1} in the second heating run (*b*). The two peaks correspond to the transition from the isotropic phase to the mesophase and from the mesophase to the isotropic phase, respectively. The mesophase, is assigned as a nematic phase based on POM and XRD studies. The glass transition temperature (T_g) of the PSI100/MEO6I complex is detected at −2°C in the second heating run. There is no crystallization peak in the cooling run.

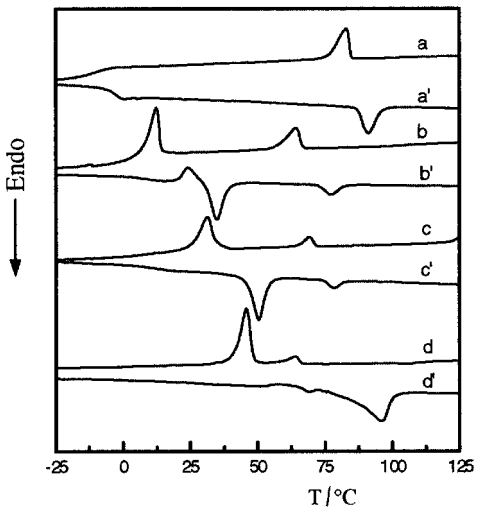

Figure 6. DSC traces of various complexes. First cooling run: (*a*) PSI100/MEO6I, (*b*) PSI100/MEO4I, (*c*) PSI100/NO6I, (*d*) PSI100/NO4I. Second heating run: (*a'*) PSI100/MEO6I, (*b'*) PSI100/MEO4I, (*c'*) PSI100/NO6I, (*d'*) PSI100/NO4I.

In contrast, there are two exothermic peaks in the cooling run of the PSI100/MEO4I complex. The peak at 65°C is attributed to the transition from the isotropic phase to the mesophase. The second peak at 12°C is attributed to the crystallization from the mesophase. In the second heating run, after a glass transition (8°C) there is a cold crystallization peak at 24°C followed by a melting peak at 35°C. The complex shows a nematic phase up to 77°C, when isotropization takes place. As the spacer length increases from 4 to 6 methylene units, the isotropization temperature increases from 77 to 91°C, but the T_g of the complex decreases from 8 to −2°C. The DSC results show that on increasing spacer length, the thermal stability of the phase and the LC temperature range both increase. The increase in the thermal stability of the LC phase is due to the decoupling function of the spacer on the motions of the polymer backbone from those of the mesogenic groups. The decrease of T_g with increasing spacer length also confirms the decoupling function of the spacer.

The complexes containing 4′-nitroazobenzene mesogenic groups—figures 6(*c*, *c'*, *d*, *d'*)—show similar trends in the thermal stability of the mesophase with increasing spacer length as the methoxyazobenzene complexes, except that no mesophase is observed in the second heating run of the PSI100/NO4I complex and a crystal phase forms below 31°C in the PSI100/NO6I complex and not in the PSI100/MEO6I complex. The monotropic nature of the mesophase of the PSI100/NO4I complex and the formation of the crystalline state by the PSI100/NO6I complex are due to the strong dipole intermolecular interactions between the 4′-nitroazobenzene mesogenic units.

The nature of the terminal group in the mesogenic unit has a profound influence on the liquid crystalline properties of the SCLCPs. For the PSI100/H6I and PSI100/H4I complexes, in which a hydrogen atom is the terminal group on the azobenzene unit, there are no exothermic peaks in the first cooling run nor endothermic peaks in the second heating run. Even cooling the complex to room temperature at 0.5°C min^{-1} does not induce any mesogenic behaviour and the complexes remain in the amorphous state throughout. Therefore,

Table 3. Transition temperatures (°C) and associated enthalpy changes (kJ mol^{-1}, in parentheses) of various equimolar complexes. I = isotropic phase; Cr = crystalline phase; N = nematic phase; g = glassy phase.

	1st cooling	2nd heating
PSI100/MEO6I	I 83(3.44) N	g −2 N 91(3.23) I
PSI100/NO6I	I 71(1.43) N 31(9.07) Cr	g 15 Cr 50(8.96) N 78(1.41) I
PSI100/MEO4I	I 65(1.74) N 12(3.02) Cr	g 8 24(2.07)[b] Cr 35(5.29) N 77(1.70) I
PSI100/NO4I	I 62(1.00) N 46(10.77) Cr	Cr 96(13.30) I

[b] Cold crystallization.

the PSI100/H6I complex and the PSI100/H4I complex are not liquid crystalline. When the terminal group is changed from nitro to methoxy, the transition temperatures T_{NI} and T_{IN} increase from 78°C and 71°C to 91°C and 83°C, respectively, while T_g decreases from 15°C to −2°C. Moreover, the crystalline state is not observed for the PSI100/MEO6I complex. The observation of a Schlieren texture shows that the nematic phase remains unaltered on cooling. The use of methoxy as the terminal group instead of nitro also leads to an increase in the associated enthalpy change, see table 3. This indicates that the replacement of the terminal hydrogen atom in the mesogenic unit by either a methoxy or nitro group stabilizes the nematic order. The higher T_{NI} (or T_{IN}) of the PSI100/MEO6I complex compared with that of the PSI100/NO6I complex, is in accordance with the order of terminal group efficiency in enhancing T_{NI} (or T_{IN}).

Van der Veen [39] suggested that if the *para*-substitutent could be easily embedded in the conjugated system, it would then contribute most to the axial polarizability of the mesogenic unit and would have a greater effect on the stabilization of the nematic order. Comparing the thermal behaviour of the complex PSI100/MEO4I with that of the PSI100/NO4I complex, a similar trend is observed, except that the latter adopts a monotropic mesogenic phase. As discussed earlier, this may be due to the strong dipolar interactions between the NO4I molecules in the PSI100/NO4I complex, which shifts T_m to a higher temperature. As a result, the melting transition overlaps the nematic–isotropic transition and the nematic mesophase becomes monotropic.

3.5. *Formation of supramolecular copolymeric complexes*

One advantage of hydrogen-bonded liquid crystalline polymers is the ease with which various 'copolymers' can be prepared. Copolymers of any desired composition can be prepared by the self-assembly of a H-bond donor polymer with a mixture of two or more different H-bond acceptors. Thus, the mesogenic properties of the copolymer can be controlled by varying the composition of the mixture of H-bond acceptors. This is in contrast to conventional systems in which separate monomers must be prepared.

Figure 7 shows the phase diagram of supramolecular copolymeric PSI100/(NO4I-MEO4I) complexes derived from PSI100 and a mixture of NO4I and MEO4I, in which the complexes are formed using a 1:1 stoichiometry of the H-bond donor and acceptor groups. The copolymeric complexes exhibit clear phase transitions and homogeneous mesophases over the entire composition range. Table 4 gives the enthalpy changes for the transition from the isotropic to nematic phase. It is

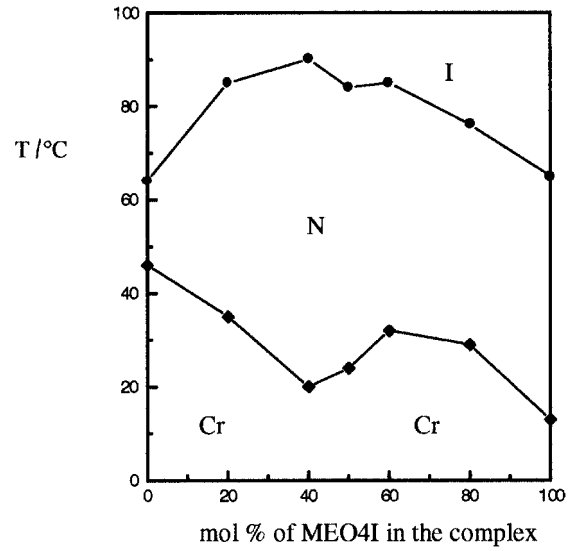

Figure 7. Phase diagram of the PSI100/(NO4I-MEO4I) system. I = isotropic phase; N = nematic phase; Cr = crystalline phase.

Table 4. Isotropic–nematic enthalpy change of copolymeric complexes shown in figure 7.

Mol fraction of MEO4I /mol %	ΔH /kJ mol^{-1}
0	1.00
20	3.86
40	4.55
50	2.79
60	3.53
80	2.62
100	1.74

difficult to determine the glass transition temperatures of the supramolecular copolymeric complexes. The phase transition temperatures of the copolymeric complexes show a significant positive deviation from ideal behaviour and are higher than those of the corresponding PSI100/NO4I and PSI100/MEO4I complexes. The enthalpy changes also show a significant positive deviation. All the copolymeric PSI100/(NO4I-MEO4I) complexes exhibit higher clearing temperatures and wider mesophase temperature ranges. POM studies and XRD measurements show that the copolymeric complexes also form a nematic phase. NO4I possesses an electron-withdrawing terminal group, and MEO4I has an electron-donating terminal group. There exists a form of electron donor–acceptor interaction between the MEO4I and NO4I units that contributes to the mesophase stabilization in the self-assembled H-bonded systems.

Schleeh *et al.* [40] have studied the mesogenic properties of conventional copolymers in which 4′-methoxyazobenzene and 4′-nitroazobenzene groups have been covalently attached to the main chain. They found that the thermal stability of the mesophase of the copolymer was enhanced and ascribed the mesophase stabilization to an electron donor–acceptor interaction between 4′-methoxyazobenze ne and 4′-nitroazobenzene. The intermolecular electron donor–acceptor interactions in the copolymer make the mesogenic units form a smectic phase. Imrie and Paterson [41] have studied the mesogenic properties of poly{4-[1-[[1-[(4-methoxyphenyl)azo]phenyl-4]oxy]-3-propyloxy]styrene} and poly{4-[1-[(4-cyanobiphenyl)-4′-oxy]-3-propyloxy]-styrene}, copolymers containing the same mesogenic groups and their analogous blends. When viewed through the microscope, although the samples were subjected to stress at temperatures slightly higher than T_g, the optical textures obtained for both polymers were insufficiently well developed to allow for phase characterization. In addition, the DSC results showed no liquid crystal–isotropic transition. However, the copolymers and the analogous blends gave clear, characteristic focal-conic fan textures indicating the formation of a smectic A phase. They attributed the formation of liquid crystallinity in the copolymers and in the blends to the specific electron donor–acceptor interaction between the unlike mesogenic units. In the present study, the synergistic cooperation of the H-bonding and the electron donor–acceptor interactions also lead to mesophase stabilization but the copolymeric supramolecular complexes form the nematic phase.

A similar result is observed for the copolymeric PSI100/(NO6I-MEO6I) complexes, as shown in figure 8. Increasing the spacer length from four to six methylene units dilutes the electron donor–acceptor interaction,

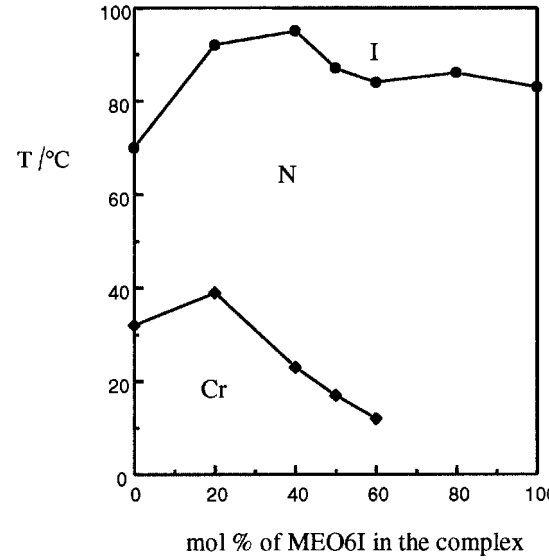

Figure 8. Phase diagram of the PSI100/(NO6I-MEO6I) system. I = isotropic phase; N = nematic phase; Cr = crystalline phase.

and hence the change of the isotropization temperature of the PSI100/(NO6I-MEO6I) complexes is less significant than that of the PSI100/(NO4I-MEO4I) complexes, see figure 9. Figure 9 shows the dependence of the increase in the phase transition temperature T_{IN} over the ideal value as calculated by a linear additivity rule using the appropriate phase transition temperatures of the PSI100/NO4I, PSI100/MEO4I, PSI100/NO6I and PSI100/MEO6I complexes.

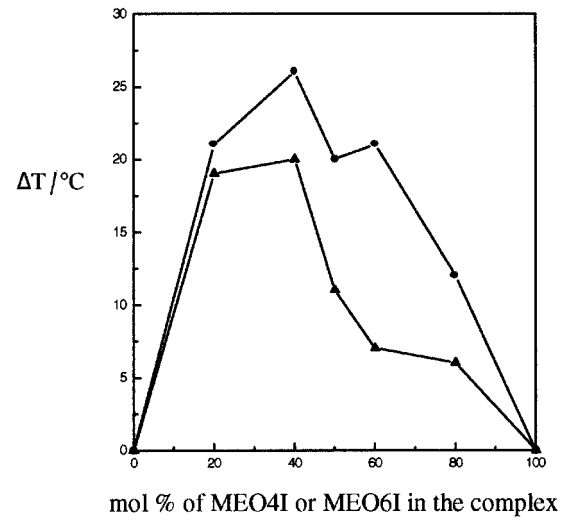

Figure 9. ΔT as a function of composition for the PSI100/(NO4I-MEO4I) (●) and PSI100/(NO6I-MEO6I) (▲) complexes. ΔT = phase transition temperature of complex (T_{IN}) − the phase transition temperature calculated using the linear additivity rule.

Figures 10 and 11 show the phase diagram of the self-assembled copolymeric complexes of PSI100/(MEO4I-H4I) and PSI100/(NO4I-H4I), respectively, while maintaining the 1:1 overall stoichiometry of the H-bond donor and acceptor moieties. The T_{IN}, T_{Cr} and T_g values for both complexes show a similar trend. On increasing the feed ratio of H4I to MEO4I or NO4I, the T_{IN}, T_{Cr} and T_g values decrease. As discussed earlier, the PSI100/H4I complex shows no LC behaviour. The existence of the H4I units in the copolymeric complexes, whose parent homopolymer shows no mesophase, dilutes the interactions between the mesogenic units, and the copolymer shows a lower clearing temperature. In other words, the interactions between the mesogenic units, NO4I or MEO4I, are stronger than those between H4I units or between MEO4I (or NO4I) and H4I units. The minimum MEO4I content required for the formation of the nematic phase in a PSI100/(MEO4I-H4I) complex is 40 mol %, whereas the PSI100/(NO4I-H4I) complexes exhibit nematic behaviour over the whole composition range examined.

From figure 10, the 'virtual' clearing temperature of the PSI100/H4I complex is estimated to be approximately −15°C by extrapolation of the clearing temperature line. If this 'virtual' clearing temperature is included in the data for the copolymeric PSI100/(NO4I-H4I) complexes, there is a positive deviation of T_{IN} over the ideal value, see figure 11. As described in the previous section, this can also be attributed to the stronger interactions between NO4I and H4I than those between MEO4I and H4I. As the dipole moment of NO4I is higher than that in MEO4I, the interaction between NO4I and H4I is stronger than that between MEO4I and H4I. When H4I is 'copolymerized' in the copolymeric complexes, the effect on the packing efficiency of the units is larger for the complexes based on NO4I. As a result, the crystallization temperatures of the PSI100/(NO4I-H4I) complexes are sharply suppressed and indeed disappear when the H4I content is above 20 mol %. On the other hand, the crystallization temperature for the copolymeric PSI100/(MEO4I-H4I) complex is no longer detected when the H4I content is above 50 mol %.

Figure 12 shows the phase diagram of the supramolecular copolymeric complexes derived from PSI100 and a mixture of MEO4I and MEO6I using a 1:1

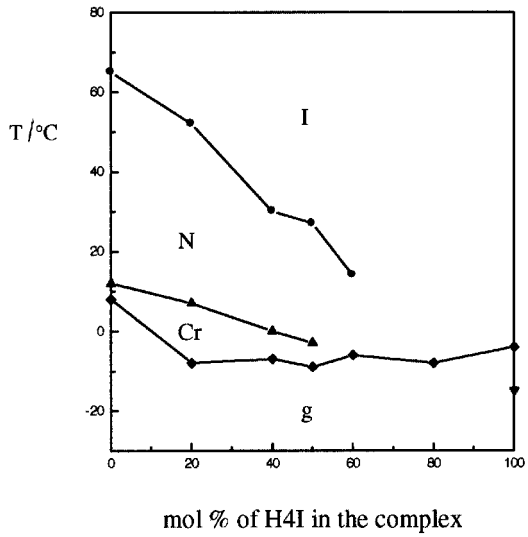

Figure 10. Phase diagram of the PSI100/(MEO4I-H4I) system. N = nematic phase; I = isotropic phase; Cr = crystalline phase; g = glass phase.

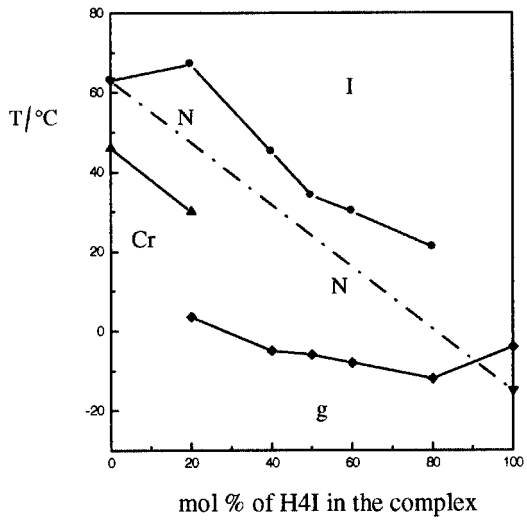

Figure 11. Phase diagram of the PSI100/(NO4I-H4I) system. N = nematic phase; I = isotropic phase; Cr = crystalline phase; g = glass phase.

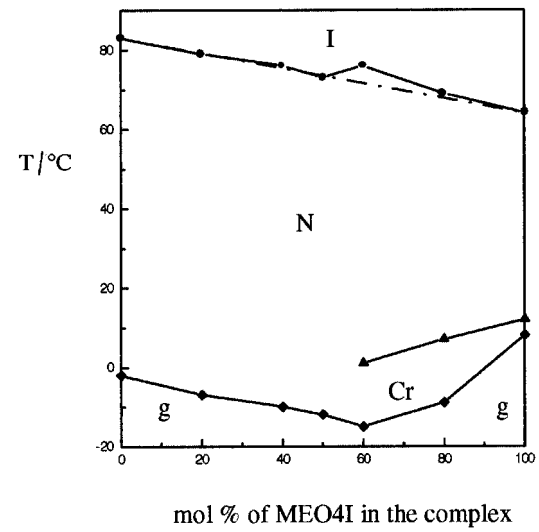

Figure 12. Phase diagram of the PSI100/(MEO4I-MEO6I) system. I = isotropic phase; N = nematic phase; Cr = crystalline phase; g = glass phase.

stoichiometry of the H-bond donor and acceptor groups. The T_{IN} temperature of the copolymeric complex changes almost linearly with copolymer composition. This is because the mesogenic units of the copolymer are identical to those of the homopolymer and the interactions between the mesogenic units in the copolymer are similar to those in the homopolymer. As such, the transition ranges of the copolymer are not significantly effected by copolymerization. The difference in the spacer length makes crystallization difficult. As a result, T_{Cr} decreases and is absent when the MEO4I content is below 60 mol %.

4. Conclusions

The formation of LC polymeric complexes arising from the self-assembly of carboxylic acid groups in PSI100 with imidazole rings in azobenzene derivatives through H-bonding has been confirmed using DSC, POM, XRD and FTIR studies. The azobenzene derivatives are attached to the polymer backbone through H-bonding, increasing the dipolar interaction between the mesogenic units. The synergistic co-operation of H-bonding and the dipolar interactions results in the formation of LC behaviour. The effects of the complex composition, the spacer length and the nature of the terminal group of the mesogenic units on the mesogenic properties are discussed. The clearing temperature and the temperature range of the LC phase increase with increasing mesogenic unit concentration and spacer length. The terminal group on the azobenzene unit plays a critical role in determining the thermal stability of the phase. While the complex does not show LC behaviour with hydrogen as the terminal group, terminal methoxy or nitro groups induce nematic behaviour near room temperature. For the supramolecular copolymeric complexes, containing a 1:1 stoichiometry of the H-bond donor polymer and the H-bond acceptor in the mixture of different azobenzene derivatives, the electron donor–acceptor interaction enhances the thermal stability of the LC phase of the complex. As a result, the mesogenic properties of the complex can be controlled by adjusting the molar ratio of the different azobenzene derivatives.

References

[1] Abe, J., Hasegawa, M., Matsushima, H., Shirai, Y., Nemoto, N., Nagase, Y., and Takamiya, N., 1995, *Macromolecules*, **28,** 2938.

[2] Imrie, C. T., Karasz, F. E., and Attard, G. S., 1994, *Macromolecules*, **27,** 1578.

[3] Bautista, M. O., Duran, R. S., and Ford, W. T., 1993, *Macromolecules*, **26,** 659.

[4] Trollsas, M., Sahlen, F., Gedde, U. W., Hult, A., Hermann, D., Rudquist, P., Komitov, L., Lagerwall, S. T., Stebler, B., Lindstrom, J., and Rydlund, O., 1996, *Macromolecules*, **29,** 2590.

[5] Ho, M. S., Natansohn, A., and Rochon, P., 1996, *Macromolecules*, **29,** 44.

[6] Meng, X., Natansohn, A., Barretl, C., and Rochon, P., 1996, *Macromolecules*, **29,** 946.

[7] Hvilsted, S., Andruzzi, F., Kulinna, C., Siesler, H. W., and Ramanujam, P. S., 1995, *Macromolecules*, **28,** 2172.

[8] Berg, R. H., Hvilsted, S., and Ramanujam, P. S., 1996, *Nature*, **383,** 505.

[9] Zhou, W., Fu, R., Dai, R., Huang, Z., and Chen, Y., 1994, *J. Chromatogr*., **659,** 477.

[10] Fu, R., Jing, P., Gu, J., Huang, Z., and Chen, Y., 1993, *Anal. Chem*., **65,** 2141.

[11] Saito, Y., Jinno, K., Pesek, J. J., Chen, Y. L., Luchr, G., Archer, J., Fetzer, J. C., and Biggs, W. R., 1993, *Chromatographia*, **38,** 295.

[12] Pesek, J. J., Lu, Y., Sioux, A., and Grandperrin, F., 1991, *Chromatographia*, **31,** 147.

[13] Kumar, U., Kato, T., and Frèchet, J. M. J., 1992, *J. Am. chem. Soc*., **114,** 6630.

[14] Kumar, U., Frèchet, J. M. J., Kato, T., Ujiie, S., and Timura, K., 1992, *Angew. Chem. int. Ed. Engl*., **31,** 1531.

[15] Kawakami, T., and Kato, T., 1998, *Macromolecules*, **31,** 4475.

[16] Kato, T., Kihara, H., Ujiie, S., Uryu, T., and Frèchet, J. M. J., 1996, *Macromolecules*, **29,** 8734.

[17] Van Nunen, J. L. M., Folmer, B. F. B., and Nolte, R. J. M., 1997, *J. Am. chem. Soc*., **119,** 283.

[18] Brandys, F. A., and Bazuin, C. G., 1996, *Chem. Mater*., **8,** 83.

[19] Malik, S., Dhal, P. K., and Mashelkar, R. A., 1995, *Macromolecules*, **28,** 2159.

[20] Alder, K. I., Stewart, D., and Imrie, C. T., 1995, *J. mater. Chem*., **5,** 2225.

[21] Stewart, D., Paterson, B. J., and Imrie, C. T., 1997, *Eur. Polym. J*., **33,** 285.

[22] Kato, T., Ihata, O., Ujiie, S., Tokita, M., and Watanabe, J., 1998, *Macromolecules*, **31,** 3551.

[23] Kato, T., Nakano, M., Moteki, T., Uryu, T., and Ujiie, S., 1995, *Macromolecules*, **28,** 8875.

[24] Lehn, J. M., 1993, *Makromol. Chem. macromol. Symp*., **69,** 1.

[25] Fouquey, C., Lehn, J. M., and Levelut, A. M., 1990, *Adv. Mater*., **2,** 254.

[26] Lin, H. C., Lin, Y. S., Chen, Y. T., Chao, I., and Li, T. W., 1998, *Macromolecules*, **31,** 7298.

[27] Ujiie, S., and Limura, K., 1992, *Macromolecules*, **25,** 3174.

[28] Wright, P. V., 1995, *J. mater. Chem*., **5,** 1275.

[29] Gohy, J. F., Vanhoorne, P., and Jèrôme, R., 1996, *Macromolecules*, **29,** 776.

[30] Percec, V., Johansson, G., Heck, J., Ungar, G., and Batty, S. V., 1993, *J. chem. Soc., Perkin Trans. 1*, 1411.

[31] Percec, V., Johansson, G., and Rodenhouse, R., 1992, *Macromolecules*, **25,** 2563.

[32] Bengs, H., Renkel, R., and Ringsdorf, H., 1991, *Makromol. Chem., rapid Commun*., **12,** 439.

[33] Ringsdorf, H., Wüstefeld, R., Zerta, E., Ebert, M., and Wendorff, J. H., 1989, *Angew. Chem. int. Ed. Engl*., **28,** 914.

[34] Li, X., Goh, S. H., Lai, Y. H., and Wee, A. T. S., 2001, *Polymer*, **42,** 5463.

[35] Luo, X. F., Goh, S. H., and Lee, S. Y., 1999, *Macromol. Chem. Phys*., **200,** 399.
[36] Imrie, C. T., Schleeh, T., Karasz, F. E., and Attard, G. S., 1993, *Macromolecules*, **26,** 545.
[37] Li, X., Goh, S. H., Lai, Y. H., and Wee, A. T. S., 2000, *Polymer*, **41,** 6563.
[38] Abe, J., Hasegawa, M., Matsushima, H., Shirai, Y., Nemoto, N., Nagase, Y., and Takamiya, N., 1995, *Macromolecules*, **28,** 2938.
[39] Van der Veen, J., de Jeu, W. H., Wanninkhof, M. W. M., and Tienhoven, C. A. M., 1973, *J. phys. Chem*., **77,** 2153.
[40] Schleeh, T., Imrie, C. T., Rice, D. M., Karasz, F. E., and Attard, G. S., 1993, *J. polym. Sci. A, polym. Chem*., **31,** 1859.
[41] Imrie, C. T., and Paterson, B. J. A., 1994, *Macromolecules*, **27,** 6673.